

Symmetrised Characterisation of Noisy Quantum Processes

Joseph Emerson,^{1,2} Marcus Silva,^{1,3} Osama Moussa,^{1,3} Colm Ryan,^{1,3} Martin Laforest,^{1,3} Jonathan Baugh,^{1,3} David G. Cory,⁴ and Raymond Laflamme^{1,3}

¹*Institute for Quantum Computing, University of Waterloo*

²*Department of Applied Mathematics, University of Waterloo*

³*Department of Physics and Astronomy, University of Waterloo*

⁴*Department of Nuclear Science and Engineering, Massachusetts Institute of Technology*

(Dated: October 31, 2018)

A major goal of developing high-precision control of many-body quantum systems is to realise their potential as quantum computers. Probably the most significant obstacle in this direction is the problem of "decoherence": the extreme fragility of quantum systems to environmental noise and other control limitations. The theory of fault-tolerant quantum error correction has shown that quantum computation is possible even in the presence of decoherence provided that the noise affecting the quantum system satisfies certain well-defined theoretical conditions. However, existing methods for noise characterisation have become intractable already for the systems that are controlled in today's labs. In this Report we introduce a technique based on symmetrisation that enables direct experimental characterisation of key properties of the decoherence affecting a multi-body quantum system. Our method reduces the number of experiments required by existing methods from exponential to polynomial in the number of subsystems. We demonstrate the application of this technique to the optimisation of control over nuclear spins in the solid state.

Quantum information enables efficient solutions to certain tasks which have no known efficient solution in the classical world. This discovery has reshaped our understanding of computational complexity and emphasized the physical nature of information. A necessary condition to take advantage of the quantum world is the ability to gain robust control of quantum systems and, in particular, counteract the noise and decoherence affecting any physical realisation of quantum information processors (QIPs). A pivotal step in this direction came with the discovery of quantum error correction codes (QECCs)[1, 2] and the associated accuracy threshold theorem for fault-tolerant (FT) quantum computation [3, 4, 5, 6]. In order to make use of quantum error correction and produce fault-tolerant protocols, we need to understand the nature of the noise affecting the system at hand. There is a direct way to fully characterise the noise using a procedure known as process tomography [7, 8, 9]. However, this procedure requires resources that grow exponentially with the number of subsystems (usually two-level systems called 'qubits'). As a result, process tomography is an intractable procedure for characterizing the multi-qubit quantum systems that have already been realised [10, 11, 12]. In this letter we introduce a general symmetrisation method that allows for direct experimental characterisation of relevant features of the noise. We apply this framework to develop an efficient experimental protocol for characterising multi-qubit correlations and memory effects in the noise. Compared to existing methods [7, 8, 9], the protocol yields an exponential savings in the number of experiments required to obtain such information. In the context of applications, this information enables tests of some key assumptions underlying estimates of the FT threshold and optimisation of error-correction strategy. Moreover, the estimated noise parameters are immediately relevant for optimizing experimental control methods. We demonstrate this optimization through an implementation of the protocol on a solid-state nuclear magnetic resonance (NMR) QIP.

We focus here on the noise affecting a system of n qubits. The crucial point is that a complete description of a general noise model Λ requires $O(2^{4n})$ parameters. Clearly an appropriate coarse-graining of this information is required; the challenge is to identify *efficient* methods for estimating the features of practical interest. The method we propose is based on identifying a symmetry associated with the properties of interest, and then operationally symmetrizing the noise process to yield an effective map $\bar{\Lambda}$ with a reduced number of independent parameters that reflect these properties (see Fig. 1). This symmetrization is achieved by conjugating the map with a unitary operator drawn from the relevant symmetry group (see Fig. 2) and then averaging with respect to that group [13, 14, 15, 16, 17]. As described below, rigorous bounds guarantee that the number of experimental trials required remains independent of the dimension of the group. Hence the randomization method leads to efficient partial characterization of the map Λ whenever the group elements admit efficient circuit decompositions.

We apply this general idea to the important problem of estimating the noise parameters that determine the performance of a broad class of QECCs and the applicability of certain assumptions underlying FT thresholds. In general, QECCs protect quantum information only against certain types of noise. A distance- $(2t + 1)$ code refers to class of codes that correct all errors simultaneously affecting up to t qubits. Hence the distance of an error correcting code determines which terms in the noise process will be corrected and which will remain uncorrected. The latter

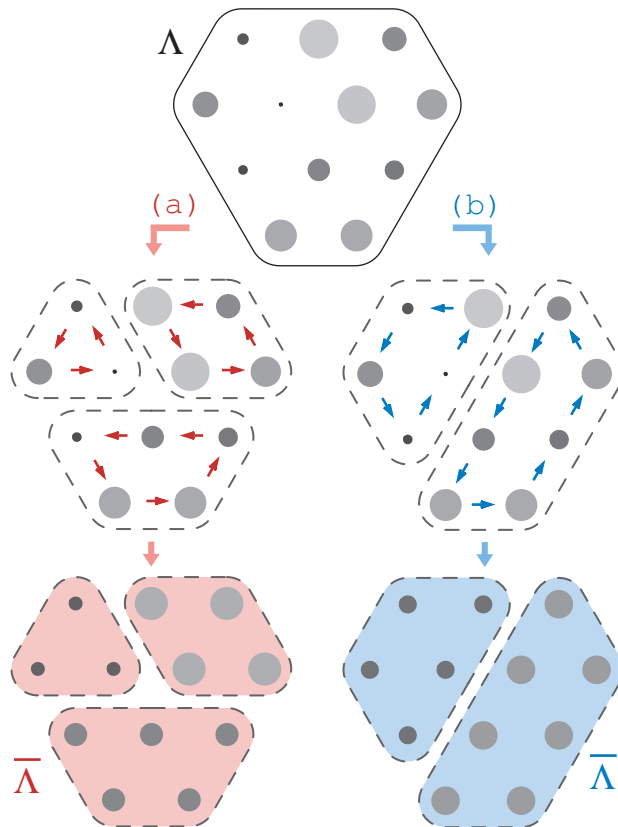


FIG. 1: **Schematic illustration of coarse-graining via symmetrization.** A general quantum process Λ is described by a finite but very large number of independent parameters (represented by shaded circles). Averaging the map by conjugation under sets of operators drawn from an appropriate symmetry group yields an effective quantum process which has a reduced number of independent parameters. In the figure we illustrate the results of two different symmetrization groups (represented by (a) red and (b) blue) which take the parameters around closed orbits. The reduced (coarse-grained) parameters of the averaged quantum process $\bar{\Lambda}$ can be determined by selecting a set of initial states ρ_i such that the output states $\bar{\Lambda}(\rho_i)$ carry a signature of the reduced parameters. In this work, we design and implement a symmetrization protocol that is relevant for characterizing the performance of quantum error correcting codes and testing some of the assumptions of fault-tolerance threshold theorems.

contribute to the overall failure probability. Of course, it is possible to estimate the failure probability under the *assumption* that the noise is independent from qubit to qubit [6] or between blocks of qubits. Many fault-tolerance theorems assume this kind of behavior. Hence a fundamental problem is to measure the correlations in the noise for a given experimental arrangement *without* the exponential overhead of process tomography. We report here a protocol that achieves this goal. We also show that this protocol remains efficient also in the context of an ensemble QIP with highly mixed states [18].

We start by expanding the noise operators in a basis of operators $P_i \in \mathcal{P}_n$, which consist of n -fold tensor product of the usual single-qubit Pauli operators $\{1, X, Y, Z\}$ satisfying the orthogonality relation $\text{Tr}[P_i P_j] = D \delta_{ij}$. The Clifford group \mathcal{C}_n is defined as the normalizer of the Pauli group \mathcal{P}_n : it consists of all elements U_i of the unitary group $U(D)$ satisfying $U_i P_j U_i^\dagger \in \mathcal{P}_n$ for every $P_j \in \mathcal{P}_n$. The protocol requires symmetrizing the channel $\Lambda \rightarrow \bar{\Lambda}$ by averaging over trials in which the channel is conjugated by the elements of \mathcal{C}_1 applied independently to each qubit (see Fig. 2). An average over conjugations is known as a “twirl” [16, 19], and hence the above is a $\mathcal{C}_1^{\otimes n}$ -twirl.

Separating out terms according to their Pauli weight w , where $w \in \{0, \dots, n\}$ is the number of non-identity factors in P_i , letting the index $\nu_w \in \{1, \dots, \binom{n}{w}\}$ count the number of distinct ways that w non-identity Pauli operators can be distributed over the n factor spaces and the index $\mathbf{i}_w = \{i_1, \dots, i_w\}$ with $i_j \in \{1, 2, 3\}$ denote which of the non-identity Pauli operators occupies the j 'th occupied site, we obtain

$$\bar{\Lambda}(\rho) = \sum_{w=0}^n \sum_{\nu_w=1}^{\binom{n}{w}} r_{w,\nu_w} \sum_{\mathbf{i}_w} P_{w,\nu_w,\mathbf{i}_w} \rho P_{w,\nu_w,\mathbf{i}_w} \quad (1)$$

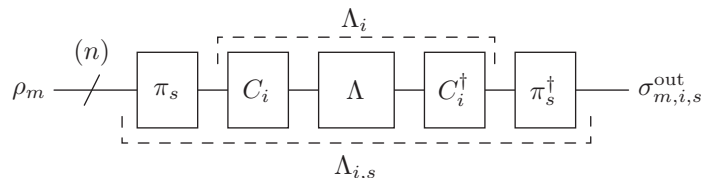


FIG. 2: **Schematic quantum circuit** for one experimental run consisting of a conjugation of the noise process Λ . Time flows from left to right. The standard protocol requires conjugation only by an element $C_i \in \mathcal{C}_1^{\otimes n}$, whereas the ensemble protocol requires conjugating Λ also by a permutation $\pi_s \in \mathcal{S}_{n,w'} \subset \mathcal{S}_n$ of the n qubits. The standard protocol requires only one (pure) input state $|0\rangle^{\otimes n}$, whereas the ensemble protocol requires n distinct input operators $\rho_{w'} = Z^{\otimes w'} \otimes \mathbb{1}^{\otimes (n-w')}$ with $w' \in \{1, \dots, n\}$. In either case the protocol involves running this circuit $k = \mathcal{O}(\log(2(n+1))/\delta^2)$ times for each input configuration to estimate the $n+1$ output parameters to precision δ with constant probability.

where $r_{w,\nu_w} = \frac{1}{3^w} \sum_{\mathbf{i}_w} a_{w,\nu_w,\mathbf{i}_w}$. (Details of this derivation are given in the appendix.) If the symmetrized channel is probed by the initial state $|0\rangle \equiv |0\rangle^{\otimes n}$, followed by a projective measurement of the output state in the basis $|l\rangle$, this yields an n -bit string $l \in \{0,1\}^n$. Let $q_{w'}$ denote the probability that a random subset of w' bits of the binary string l has even parity. Noting that $c_{w'} \equiv \langle Z^{\otimes w'} \rangle = 2q_{w'} - 1$, where $\langle Z^{\otimes w'} \rangle$ is the average of all Pauli operators with w' factors of Z and $n-w'$ identity factors, we obtain $p_w = \sum_{w'} \Omega_{w,w'}^{-1} c_{w'}$ where the matrix $\Omega_{w,w'}^{-1}$ is a matrix of combinatorial factors given in the appendix, and the p_w are the probabilities of w simultaneous qubit errors occurring over the course of the quantum process. Of course all imperfections in the protocol contribute to the total probabilities of error. The protocol can be made robust against imperfections in the input state preparation, measurement and twirling by substituting $c_{w'} \rightarrow \tilde{c}_{w'} = c_{w'} / \langle Z^{\otimes w'} \rangle_0$, where we simply factor out the expectation value observed when the protocol is performed without the noisy channel. In this case the probabilities of different error weights are given by $p_w = \sum_{w'} \Omega_{w,w'}^{-1} \tilde{c}_{w'}$.

If in each single shot experiment the Clifford operators are chosen uniformly at random then with $K = \mathcal{O}(\log(2(n+1))/\delta^2)$ experiments we can estimate each of the coefficients c_w to precision δ with constant probability. The $c_{w'}$ can be applied directly to test some of the assumptions that yield rigorous estimates of the fault-tolerance threshold [20]. In particular, a noisy channel with an uncorrelated distribution of error locations, but with arbitrary correlations in the error type at each location, is mapped under our symmetrization to a channel which is a tensor product of n single-qubit depolarizing channels. A channel satisfying this property will exhibit the scaling $c_w = c_1^w$. Hence observed deviations from this scaling law imply a violation of the above assumption. Furthermore, the question of whether the noise exhibits non-Markovian properties can be tested efficiently by repeating the above scheme for distinct time-intervals $m\tau$ with increasing m . Markovian noise is guaranteed to satisfy the semi-group property $\bar{\Lambda}_{\tau_1} \circ \bar{\Lambda}_{\tau_2} = \bar{\Lambda}_{\tau_1+\tau_2}$, and hence memory effects in the noise are implied by any observed deviations from the condition $c_w(m\tau) = (c_w(\tau))^m$.

The estimates $c_{w'}$ also give estimates for p_w , but the statistical uncertainty for p_w grows exponentially with w . Using a bound on $\Omega_{w,w'}^{-1}$ derived in the appendix, we show that all p_w for which $w \leq l$ can be estimated with $\mathcal{O}(n^l)$ trials. This allows for characterisation of other important features of the noise. The probability p_0 is directly related to the entanglement fidelity of the channel and hence this protocol provides an exponential savings over recently proposed methods for estimating this single figure of merit [15, 21, 22] (see also Ref. [16]). Hence, by actually implementing any given code we can bound the failure probability of that code with only $\mathcal{O}(\log(2n)/\delta^2)$ experiments without making any theoretical assumptions about the noise. Moreover, on physical grounds we may expect the noise to become independent between qubits outside some fixed (but unknown) scale b , after which the p_w decrease exponentially with w . The scale b can be determined efficiently with n^b experiments.

While a characterisation of the twirled channel is useful given the relevance of twirled channels to fault-tolerant applications [23, 24], we remark that the failure probability of the twirled channel gives an upper bound to the failure probability of the original un-twirled channel whenever the performance of the code has some bound that is invariant under the symmetry associated with the twirl. This holds quite generally in the context of the symmetry considered above because the failure probability of a generic distance- $2t+1$ code is bounded above by the total probability of error terms with Pauli weight greater than t and this weight remains invariant under conjugation by any element $C_i \in \mathcal{C}_1^{\otimes n}$.

Our method provides an efficient protocol for the characterisation of the noise in contexts where the target transformation is the identity operator, e.g. a quantum communication channel or quantum memory. However, the protocol also provides an efficient means for characterising the noise under the action of a non-identity unitary transformation such as a quantum gate. There are two ways to adapt the protocol to this setting. First, we recall that a unitary transformation can be decomposed into a product of basic quantum gates drawn from a universal gate set, where

each gate in the set acts on at most 2 qubits simultaneously. Hence, the noise map acting on all n qubits associated with any 2-qubit gate can be determined by applying the above protocol to other $n - 2$ qubits while applying process tomography to the 2 qubits in the domain of the quantum gate. A second approach is to estimate the average error-per-gate for a sequence of m gates such that the composition gives the identity operator. Such a sequence can be generated by making use of the cyclic property $U^m = 1$ of any gate in a universal gate set, or by choosing a sequence of $m - 1$ random gates followed by an m 'th gate chosen such that the composition gives the identity transformation [25].

#	System	Map Description	Kraus operators (A_k)	k	p_0	p_1	p_2	p_3
1	CHCl ₃	Engineered: $\mathbf{p} = [0, 1, 0]$.	$\frac{1}{\sqrt{2}}\{Z_1, Z_2\}$	288	0.000 ^{+0.004} _{-0.001}	0.991 ^{+0.009} _{-0.015}	0.009 ^{+0.017} _{-0.009}	-
2	CHCl ₃	Engineered: $\mathbf{p} = [0, 0, 1]$.	$\{Z_1 Z_2\}$	288	0.001 ^{+0.006} _{-0.001}	0.004 ^{+0.011} _{-0.004}	0.996 ^{+0.004} _{-0.011}	-
3	CHCl ₃	Engineered: $\mathbf{p} = [\frac{1}{4}, \frac{1}{2}, \frac{1}{4}]$.	$\{\exp[i\frac{\pi}{4}(Z_1 + Z_2)]\}$	288	0.254 ^{+0.010} _{-0.010}	0.495 ^{+0.021} _{-0.020}	0.250 ^{+0.019} _{-0.019}	-
4	C ₃ H ₄ O ₄	Engineered: $\mathbf{p} = [0, 1, 0, 0]$.	$\frac{1}{\sqrt{3}}\{Z_1, Z_2, Z_3\}$	432	0.01 ^{+0.01} _{-0.01}	0.99 ^{+0.01} _{-0.03}	0.01 ^{+0.02} _{-0.01}	0.00 ^{+0.01}
5	C ₃ H ₄ O ₄	Natural noise (a)	unknown	432	0.44 ^{+0.01} _{-0.02}	0.45 ^{+0.03} _{-0.03}	0.10 ^{+0.04} _{-0.08}	0.01 ^{+0.03} _{-0.01}
6	C ₃ H ₄ O ₄	Natural noise (b)	unknown	432	0.84 ^{+0.01} _{-0.01}	0.15 ^{+0.02} _{-0.03}	0.01 ^{+0.03} _{-0.01}	0.00 ^{+0.02}

TABLE I: **Summary of experimental results.** The first four sets of experiments (three sets on the two-qubit liquid-state system, and one on the three-qubit solid-state system) were designed to characterise the performance of the protocol under engineered noise. The last two sets were designed to characterize the (unknown) natural noise due to imperfect averaging of the internal Hamiltonian terms under a multiple-pulse time-suspension sequence [26] with (a) one cycle with $10\mu s$ pulse-spacing, and (b) two cycles with $5\mu s$ pulse-spacing. The latter experiments characterized the residual errors under the sequence with respect to the particular symmetry implemented by the twirling process. The results of the solid-state experiments are calculated after factoring out the effect of decoherence occurring during the twirling operations (which only accounted for $\simeq 1\%$ fidelity loss per gate) in order to isolate the noise associated with the time-suspension sequence.

We now describe how the above protocol is efficient also in the context of an ensemble QIP [18]. First, we prepare deviations from the identity state of the form $\rho_{w'} = Z^{\otimes w'} \otimes \mathbb{1}^{\otimes(n-w')}$ with $w' = \{1, \dots, n\}$. Hence the (non-scalable) preparation of pseudo-pure states is not required. Second, we directly measure $\langle Z^{\otimes w'} \rangle$ for each w' from the expectation value $\langle Z^{\otimes w'} \mathbb{1}^{\otimes(n-w')} \rangle$ by explicitly performing a random permutation of the qubits. Let $\mathcal{S}_{n,w'}$ denote any subset of the group of permutations of n qubits, \mathcal{S}_n , such that $\sum_s \pi_s \rho_{w'} \pi_s^\dagger = \sum_{\nu_{w'}} \rho_{w',\nu_{w'}}$, where $\nu_{w'} \in \{1, \dots, \binom{n}{w'}\}$ denotes each distribution of the w' Z -Pauli operators. As illustrated in Fig. 2, the symmetrisation consists of conjugating the process Λ with $C_i \in \mathcal{C}_1^{\otimes n}$ and $\pi_s \in \mathcal{S}_{n,w'}$. Let $\Lambda_{i,s}$ stand for the conjugated noise-map, then, given input operator $\rho_{w'}$, the output is $\sigma_{w',i,s}^{\text{out}} = \Lambda_{i,s}(\rho_{w'})$. Averaging the output operators $\sigma_{w',i,s}^{\text{out}}$ over i and s gives the input operator scaled by $c_{w'}$.

We illustrate an implementation of the above protocol on both a 2-qubit (chloroform CHCl₃) liquid-state and a 3-qubit (single-crystal Malonic acid C₃H₄O₄) solid-state NMR QIP (see the appendix for more information on methods). The results of six sets of experiments are summarized in Table I, and detailed results for one liquid-state set are shown in Fig. 3 and for two solid-state sets are shown in Fig. 4. The first four sets of experiments were performed under engineered noise to both characterize the performance of the protocol and to confirm high-fidelity control. Two final two sets of experiments were performed in the solid-state to characterize the unknown residual noise occurring under (a) one cycle of a C48 pulse sequence [26] with $10\mu s$ pulse spacing, and (b) two cycles of C48 with $5\mu s$ pulse spacing. The C48 sequence is designed to suppress the dynamics due to the system's internal Hamiltonian. The evolution of the system under this pulse sequence can be evaluated theoretically by calculating the Magnus expansion [27] of the associated effective Hamiltonian, under which the residual effects appear as a sum of terms associated with the Zeeman and dipolar parts of the Hamiltonian, including cross terms. Roughly speaking, effective suppression of the k^{th} term of the Hamiltonian takes places when $\gamma_k \tau_k \ll 1$, where γ_k is the strength of the term and τ_k^{-1} is the rate at which it is modulated by the pulse sequence. Generally shorter delays lead to improved performance unless there is a competing process at the shorter time-scale or there are limitations due to pulse imperfections. Hence the performance of the pulse sequence is best evaluated via experimental characterisation. The results shown in Table I and Fig. 4 illustrate how the protocol can compare the performance of the two multiple-pulse time-suspension sequences both in terms of the overall fidelity and in terms of the relative probability of one, two and three body noise terms.

The method above is an illustration of the first step in a hierarchy of tests that are available under the general approach, with each test giving more fine-grained information. For example, a variation of the protocol in which only a Pauli-twirl is applied enables a estimation of the $\mathcal{O}(n^3)$ relative probabilities of Pauli X , Y and Z errors. This

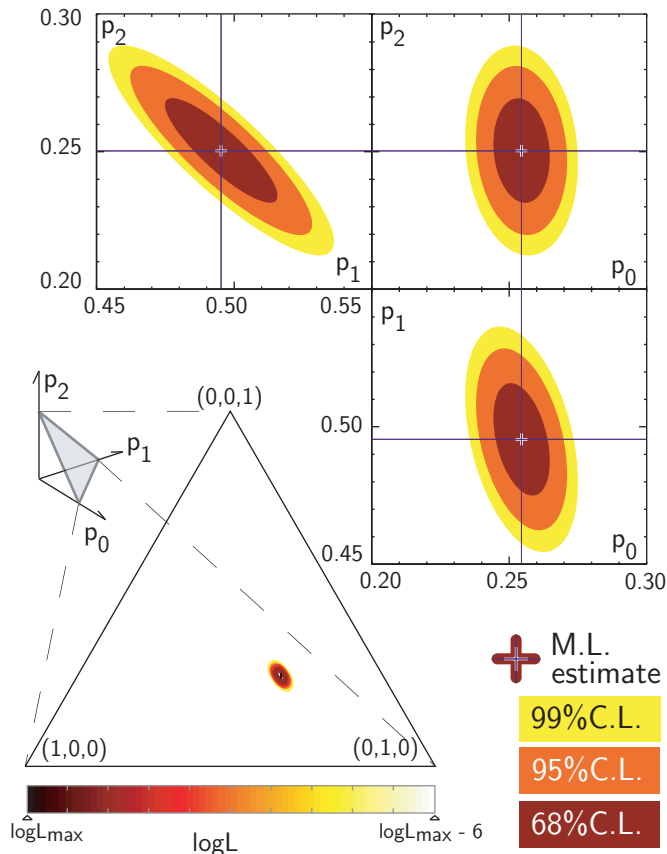


FIG. 3: **Results for experiment #3 in Table I.** Shown is the Maximum Likelihood (ML) estimate, $\mathbf{p}_{exp} = [0.254^{+0.010}_{-0.010}, 0.495^{+0.021}_{-0.020}, 0.250^{+0.019}_{-0.019}]$, for the error probabilities of the engineered noise, $A_1 = \{\exp[-i\frac{\pi}{4}(Z_1 + Z_2)]\}$, for which the calculated values are $\mathbf{p} = [\frac{1}{4}, \frac{1}{2}, \frac{1}{4}]$. Also shown are the confidence regions for the 68%, 95%, and 99% confidence levels (C.L.), which can be determined from the log of a likelihood function, $\log L$. The experiment was performed on a 2-qubit liquid-state NMR processor, and the noise was implemented by appropriately phase-shifting the pulses. These experiments illustrate the precision with which the protocol can be implemented under conditions of well-developed quantum control.

more fine-grained information is useful not only for optimisation over QECC in eventual applications, but also to characterize current performance of a given experimental set-up. The full scope of information that can be estimated efficiently via this general symmetrisation approach is an important topic for further research. A specific question in this direction is to determine whether this approach might enable efficient detection of the presence of noiseless subsystems.

APPENDIX A: ANALYSIS OF THE SYMMETRISATION

The generic noise affecting a quantum state ρ (a positive matrix of dimension $D \times D$) can be represented by a completely positive map of the form $\Lambda(\rho) = \sum_{k=1}^{D^2} A_k \rho A_k^\dagger$, which is normally subject to a trace-preserving condition $\sum_k A_k^\dagger A_k = 1$. We focus here on systems of n qubits so that $D = 2^n$.

We start by expanding the noise operators in a basis of Pauli operators $P_i \in \mathcal{P}_n$ consists of n -fold tensor product of the usual single-qubit Pauli operators $\{1, X, Y, Z\}$, giving $A_k = \sum_{i=1}^{D^2} \alpha_i^{(k)} P_i / \sqrt{D}$, where $\alpha_i^{(k)} = \text{Tr}[A_k P_i] / \sqrt{D}$, and the Pauli's satisfy the orthogonality relation $\text{Tr}[P_i P_j] = D \delta_{ij}$. The Clifford group \mathcal{C}_n is defined as the normalizer of the Pauli group \mathcal{P}_n : it consists of all elements U_i of the unitary group $U(D)$ satisfying $U_i P_j U_i^\dagger \in \mathcal{P}_n$ for every $P_j \in \mathcal{P}_n$.

We can analyze the effect of the twirl $\mathcal{C}_1^{\otimes n}$ by noting that any element $C_i \in \mathcal{C}_1^{\otimes n}$ can be expressed as $C_i = P_j Y_l$, where $P_j \in \mathcal{P}_n$ and $Y_l \in \mathcal{Y}_1^{\otimes n}$, and where we consider as equivalent elements of each group that differ only by a phase.

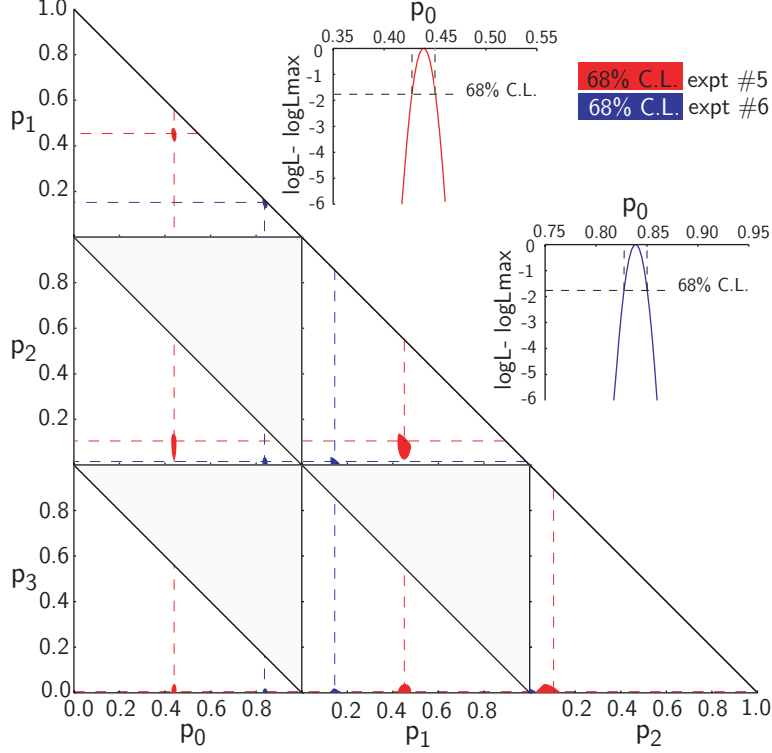


FIG. 4: **Results for experiments #5 and #6 in Table I.** Shown are projections of the 4-dimensional likelihood function onto various probability planes. The asymmetry seen in some of the confidence areas is a result of this projection. The results for one cycle with $10\mu\text{s}$ pulse-spacing (exp #5) are in red and the results for two cycles with $5\mu\text{s}$ spacing (exp #6) are in blue. The rate set by a pulse-spacing of $10\mu\text{s}$ leads to a poor overall fidelity for the time-suspension sequence, and, in particular, a significant probability of two-qubit errors from the residual terms in the effective Hamiltonian. Under two repetitions of the sequence with the pulse-spacing of $5\mu\text{s}$ (which has twice as many pulses as the single sequence with the $10\mu\text{s}$ spacing), the probability of two-qubit errors in the residual terms decreases substantially. The overall fidelity of either pulse-sequence is still limited by incomplete heteronuclear decoupling of the qubits (carbon nuclei) from the environment (nearby hydrogen nuclei): at the $5\mu\text{s}$ pulse-spacing the carbon nuclei are being modulated on a time-scale close to the proton decoupling frequency, so that the decoupling sequence no longer averages the heteronuclear coupling to zero. A simple extension of the protocol allows for determining which qubit accrues the greatest single qubit errors from this effect. The results were consistent with identifying the primary source of single-qubit errors as the qubit whose coupling to the hydrogen is an order of magnitude larger than that of the other two. By increasing the decoupling power we were able to reduce these errors though they could not be removed completely due to hardware limitations.

Hence, the $\mathcal{C}_1^{\otimes n}$ -twirl of an arbitrary channel Λ consists of the action

$$\Lambda(\rho) \rightarrow \overline{\Lambda(\rho)} = \frac{1}{|\mathcal{C}_1^{\otimes n}|} \sum_{j=1}^{|\mathcal{S}_1^{\otimes n}|} \sum_{l=1}^{|\mathcal{P}_n|} \sum_k S_j^\dagger P_l^\dagger A_k P_l S_j \rho S_j^\dagger P_l^\dagger A_k^\dagger P_l S_j. \quad (2)$$

where $|\mathcal{C}_1^{\otimes n}| = |\mathcal{S}_1^{\otimes n}| |\mathcal{P}_n|$. The effect of the Pauli-twirl is to create the channel $\sum_i a_i P_i \rho P_i$, where $a_i = \sum_k |\alpha_i^{(k)}|^2 / D$ are probabilities, known as a Pauli channel. The effect of the symplectic-twirl on the Pauli channel is to map each of the non-identity Pauli operators to a uniform sum over the 3 non-identity Pauli operators. To express this we separate out terms according to their Pauli weight w , where $w \in \{0, \dots, n\}$ is the number of non-identity factors in P_l . We let the index $\nu_w \in \{1, \dots, \binom{n}{w}\}$ count the number of distinct ways that w non-identity Pauli operators can be distributed over the n factor spaces, and the index $\mathbf{i}_w = \{i_1, \dots, i_w\}$ with $i_j \in \{1, 2, 3\}$ denote which of the non-identity Pauli operators occupies the j 'th occupied site. Hence we have,

$$\overline{\Lambda(\rho)} = \frac{1}{|\mathcal{S}_1^{\otimes n}|} \sum_{j=1}^{|\mathcal{S}_1^{\otimes n}|} \sum_{w=0}^n \sum_{\nu_w=1}^{\binom{n}{w}} \sum_{\mathbf{i}_w=1}^{3^w} a_{w,\nu_w,\mathbf{i}_w} S_j^\dagger P_{w,\nu_w,\mathbf{i}_w} \rho S_j P_{w,\nu_w,\mathbf{i}_w} S_j. \quad (3)$$

Now, for any term with arbitrary but fixed w and ν_w , we have the expression,

$$\frac{1}{|\mathcal{S}_1^{\otimes n}|} \sum_{\mathbf{i}_w=1}^{3^w} a_{w,\nu_w,\mathbf{i}_w} \sum_{j=1}^{|\mathcal{S}_1^{\otimes n}|} S_j^\dagger P_{w,\nu_w,\mathbf{i}_w} S_j \rho S_j^\dagger P_{w,\nu_w,\mathbf{i}_w} S_j = \left(\frac{1}{3^w} \sum_{\mathbf{i}_w}^{3^w} a_{w,\nu_w,\mathbf{i}_w} \right) \sum_{\mathbf{j}_w=1}^{3^w} P_{w,\nu_w,\mathbf{j}_w} \rho P_{w,\nu_w,\mathbf{j}_w}. \quad (4)$$

Consequently we obtain,

$$\overline{\Lambda(\rho)} = \sum_{w=0}^n \sum_{\nu_w=1}^{\binom{n}{w}} r_{w,\nu_w} \sum_{\mathbf{i}_w=1}^{3^w} P_{w,\nu_w,\mathbf{i}_w} \rho P_{w,\nu_w,\mathbf{i}_w} \quad (5)$$

where $r_{w,\nu_w} = \frac{1}{3^w} \sum_{\mathbf{i}_w=1}^{3^w} a_{w,\nu_w,\mathbf{i}_w}$. If we explicitly apply random qubit permutations chosen uniformly, then the effective channel $\overline{\Lambda}^\Pi$ is given by

$$\overline{\Lambda}^\Pi(\rho) = \sum_{w=0}^n p_w \sum_{\nu_w=1}^{\binom{n}{w}} \sum_{\mathbf{i}_w=1}^{3^w} \frac{1}{3^w \binom{n}{w}} P_{w,\nu_w,\mathbf{i}_w} \rho P_{w,\nu_w,\mathbf{i}_w}, \quad (6)$$

where

$$p_w = 3^w \sum_{\nu_w=1}^{\binom{n}{w}} r_{w,\nu_w}. \quad (7)$$

This symmetrized channel can now be probed experimentally by inputting the initial state $|0\rangle \equiv |0\rangle^{\otimes n}$ and performing a projective measurement in the computational basis $|l\rangle$, where $l \in \{0,1\}^n$. If we distinguish outcome bit strings only according to their Hamming weight $h \in 0, \dots, n$, the effect is equivalent to a random permutation of the qubits. Observe that only Pauli X and Y errors will affect the Hamming weight because Pauli Z errors commute with the input state. Hence the probability of measuring an outcome with Hamming weight h is

$$u_h = \sum_{w=0}^n R_{hw} p_w$$

where $R_{hw} = \binom{w}{h} 2^h / 3^w$ gives the number of Pauli operators of weight w of which exactly h are either X or Y , and where

$$p_w = 3^w \sum_{\nu_w=1}^{\binom{n}{w}} r_{w,\nu_w} = \sum_{\nu_w=1}^{\binom{n}{w}} \sum_{\mathbf{i}_w}^{3^w} p_{w,\nu_w,\mathbf{i}_w} \quad (8)$$

is a quantity of interest, i.e., the total probability of all Pauli errors with weight w . Noting that the $n \times n$ matrix R_{hw} satisfies $R_{hw} = 0$ when $h > w$ and hence is upper triangular, estimates of the p_w can be recovered trivially from the measured probabilities u_h after n back-substitutions. In another approach, if we distinguish outcome bit strings only by the parity of a random subset of w qubits, then the effect is also equivalent to a random permutation of the qubits. Thus, experimentally we implement $\overline{\Lambda(\rho)}$ via twirling, but access the parameters of $\overline{\Lambda}^\Pi(\rho)$ by averaging over random choices of subsets of w qubits. The probability q_w that the parity of random subset of w qubits is even is related to $\langle \overline{Z^{\otimes w}} \rangle$ via

$$c_w \equiv \langle \overline{Z^{\otimes w}} \rangle = q_w - (1 - q_w) = 2q_w - 1, \quad (9)$$

where we have defined the variable c_w for ease of notation. In order to analyze the information content of the c_w and their relation to the error probabilities p_w it is convenient to consider the Liouville representation of the twirled channel.

Liouville Representation of the Twirled Channel

Because any two operators $P_{m,\nu_m,\mathbf{i}_m} \in \mathcal{P}_n$ either commute or anti-commute, it follows that

$$\overline{\Lambda}^\Pi(P_{m,\nu_m,\mathbf{i}_m}) = (\text{Pr}(\text{comm}) - \text{Pr}(\text{anti-comm})) P_{m,\nu_m,\mathbf{i}_m} = c_m P_{m,\nu_m,\mathbf{i}_m}, \quad (10)$$

where $\text{Pr}(\text{comm})$ ($\text{Pr}(\text{anti-comm})$) is the probability of the channel $\bar{\Lambda}^\Pi$ acting with a noise operators P_{w,ν_w,\mathbf{i}_w} which commutes (anti-commutes) with P_{m,ν_m,\mathbf{i}_m} . Thus, the Pauli operators P_{m,ν_m,\mathbf{i}_m} are the eigenoperators of the channel with corresponding eigenvalues c_m . The eigendecomposition of $\bar{\Lambda}^\Pi$ is given by

$$\bar{\Lambda}^\Pi(\rho) = \sum_{w=0}^n c_w M_w^c(\rho), \quad (11)$$

where M_w^c are the superoperators

$$M_w^c(\rho) = \frac{1}{2^n} \sum_{\nu_w=0}^{\binom{n}{w}} \sum_{\mathbf{i}_w=0}^{3^w} P_{w,\nu_w,\mathbf{i}_w} \text{tr}(P_{w,\nu_w,\mathbf{i}_w} \rho). \quad (12)$$

We can also rewrite the usual parameterisation of $\bar{\Lambda}^\Pi$ as

$$\bar{\Lambda}^\Pi(\rho) = \sum_{w=0}^n p_w M_w^p(\rho), \quad (13)$$

where M_w^p are the superoperators

$$M_w^p(\rho) = \frac{1}{3^w \binom{n}{w}} \sum_{\nu_w=0}^{\binom{n}{w}} \sum_{\mathbf{i}_w=0}^{3^w} P_{w,\nu_w,\mathbf{i}_w} \rho P_{w,\nu_w,\mathbf{i}_w}. \quad (14)$$

By considering the Liouville representation of these superoperators it is easy to show that the M_w^c are orthogonal and that the M_w^p are orthogonal. Thus, $\{c_w\}_{w=0}^n$ parameterizes the channel $\bar{\Lambda}^\Pi$ uniquely, and $\{p_w\}_{w=0}^n$ also parameterizes the same channel uniquely. Using the Liouville representation it follows that these parameterizations are related by a $(n+1) \times (n+1)$ matrix Ω such that

$$c_w = \sum_{w'=0}^n p_{w'} \Omega_{w,w'}, \quad (15)$$

$$p_w = \sum_{w'=0}^n c_{w'} \Omega_{w,w'}^{-1} \quad (16)$$

with Ω defined by

$$\Omega_{w,w'} = \frac{4^n}{3^{w+w'} \binom{n}{w} \binom{n}{w'}} \langle M_w^c, M_{w'}^p \rangle \quad (17)$$

$$\Omega_{w,w'}^{-1} = \langle M_{w'}^p, M_w^c \rangle, \quad (18)$$

where $\langle \cdot, \cdot \rangle$ is the Hilbert-Schmidt inner product of superoperators acting on Liouville space defining the notion of orthogonality discussed above. To obtain an explicit expression for $\Omega_{w,w'}$, we start from (10) and observe that a Pauli operator of weight w is scaled by a channel of the form

$$\mathcal{N}_{w'}(\rho) = \frac{1}{3^{w'} \binom{n}{w'}} \sum_{\nu_{w'}=0}^{\binom{n}{w'}} \sum_{\mathbf{i}_{w'}=0}^{3^{w'}} P_{w',\nu_{w'},\mathbf{i}_{w'}} \rho P_{w',\nu_{w'},\mathbf{i}_{w'}}. \quad (19)$$

This implies

$$\Omega_{m,w} = -1 + \sum_{L=\max(0,w+m-n)}^{\min(m,w)} \frac{\binom{n-m}{w-L} \binom{m}{L} 3^L + (-1)^L}{\binom{n}{w}} \frac{1}{3^L}, \quad (20)$$

and, using (17) and (18), it follows that

$$\Omega_{m,w}^{-1} = \frac{3^{m+w} \binom{n}{m} \binom{n}{w}}{4^n} \Omega_{m,w}. \quad (21)$$

Simple examples

For the case of two-qubit channels, this matrix is given by

$$\Omega = \begin{pmatrix} 1 & 1 & 1 \\ 1 & \frac{1}{3} & -\frac{1}{3} \\ 1 & -\frac{1}{3} & \frac{1}{9} \end{pmatrix} \quad (22)$$

$$\Omega^{-1} = \frac{1}{16} \begin{pmatrix} 1 & 6 & 9 \\ 6 & 12 & -18 \\ 9 & -18 & 9 \end{pmatrix}, \quad (23)$$

and for the case of three-qubit channels, it is given by

$$\Omega = \begin{pmatrix} 1 & 1 & 1 & 1 \\ 1 & \frac{5}{9} & \frac{1}{9} & -\frac{1}{3} \\ 1 & \frac{1}{9} & -\frac{5}{27} & \frac{1}{9} \\ 1 & -\frac{1}{3} & \frac{1}{9} & -\frac{1}{27} \end{pmatrix} \quad (24)$$

$$\Omega^{-1} = \frac{1}{64} \begin{pmatrix} 1 & 9 & 27 & 27 \\ 9 & 45 & 27 & -81 \\ 27 & 27 & -135 & 81 \\ 27 & -81 & 81 & -27 \end{pmatrix} \quad (25)$$

APPENDIX B: UNCORRELATED NOISE LOCATIONS

A noise channel over n qubits that has a distribution of error locations which is uncorrelated, but otherwise arbitrary, is mapped under twirling and random permutations to a channel which is a tensor product of n single-qubit depolarizing channels. Each of these single-qubit channels has the form

$$\mathcal{D}(\rho) = (1-p)\rho + \frac{p}{3}(X\rho X + Y\rho Y + Z\rho Z) \quad (26)$$

and scales a single-qubit Pauli operator by $c_1 = 1 - \frac{4}{3}p$. Thus, the n qubit channel will scale a Pauli operator with weight w by $c_w = c_1^w$.

Due to the finite accuracy with which the eigenvalues c_w are estimated through experiment, we can only impose this as a necessary condition for the independence of the distribution of error locations. Therefore, any estimate of the eigenvalues which makes such an exponential dependence unlikely, also implies that the distribution of the error locations is unlikely to be uncorrelated.

APPENDIX C: STATISTICAL ANALYSIS

The circuit complexity is depth 2 with only $2n$ single-qubit gates required for the protocol. The outcome from any single experiment is just a binary string. The number of such trials required to estimate the probability $q_{w'}$ of even parity for a random subset of w' bits to within a given precision δ is clearly independent of the number of qubits because the problem is reduced to the simple task of estimating the probability of a 2-outcome classical statistical test. More precisely from the Chernoff inequality, any estimate of the exact average $\mathbb{E}[X] = q_w$ after K *independent trials* satisfies,

$$\Pr\left(\left|\frac{1}{K} \sum_{i=1}^K X_i - \mathbb{E}[X]\right| > \delta\right) \leq 2 \exp(-\delta^2 K). \quad (27)$$

We see that the number of experiments required to estimate q_w to precision δ with constant probability is at most,

$$K = \log(2)\delta^{-2},$$

where each experiment is an *independent trial* consisting of a single shot experiment in which the Clifford gates are chosen uniformly at random. The number of experimental trials required to estimate the complete set of probabilities $\{q_0, \dots, q_w, \dots, q_n\}$ can be obtained from the union bound,

$$\Pr(\cup_w \mathcal{E}_w) \leq \sum_w \Pr(\mathcal{E}_w) \quad (28)$$

which applies for arbitrary events \mathcal{E}_w . In our case each \mathcal{E}_w is associated with the event that $|\frac{1}{K} \sum_{k=1}^K X_k - \mathbb{E}[X]| > \delta$ and similarly $\cup_w \mathcal{E}_w$ is the probability that at least one of the $n+1$ estimated probabilities q_w satisfies this property (i.e., is an unacceptable estimate) after K trials. Whence, the probability that at least one of the $n+1$ estimated probabilities is outside precision δ of the exact probability is bounded above by,

$$\Pr(\cup_w \mathcal{E}_w) \leq 2(n+1) \exp(-\delta^2 K).$$

This implies that at most $K = \mathcal{O}(\delta^{-2} \log(2(n+1)))$ experimental trials are required to estimate each of the components of the (probability) vector (q_0, \dots, q_n) to within precision δ with constant probability.

Uncertainty of p_w Estimates

Given an estimate of the $c_w = \langle Z^{\otimes w} \rangle$ with some variance σ^2 , the variance of the estimate of a particular p_w is given by

$$\sigma_w^2 = \sum_{i=0}^n \sum_{j=0}^n \Omega_{w,i}^{-1} \Omega_{w,j}^{-1} \text{Cov}(c_i, c_j) \quad (29)$$

Assuming the estimates for all c_w have the same variance, the positivity constraint on the covariance matrix of the c_w estimates requires that $|\text{Cov}(c_i, c_j)| \leq \sigma^2$, yielding the upper bound

$$\sigma_w^2 \leq \sigma^2 \sum_i \sum_j |\Omega_{w,i}^{-1} \Omega_{w,j}^{-1}|. \quad (30)$$

From (10), it is clear that

$$|\Omega_{w,w'}| \leq 1, \quad (31)$$

so the from (21) we have

$$\sigma_w \leq \sigma 3^w \binom{n}{w}. \quad (32)$$

Using the fact that

$$\binom{n}{w} \leq \frac{n^w e^w}{w^w}, \quad (33)$$

we can rigorously show that the uncertainty σ_w on the estimate of p_w is bounded by

$$\sigma_w \leq \sigma \left(\frac{3}{w}\right)^w n^w e^w. \quad (34)$$

Exact numerical computation of the uncertainty scaling factor $\frac{\sigma_w}{\sigma}$, depicted in Figure 5, indicates that for fixed w the uncertainty grows as a polynomial in n , but the degree of that polynomial depends linearly on w . For large n , we find that

$$\frac{\sigma_w}{\sigma} \approx e^{kw+a} n^{mw+b}, \quad (35)$$

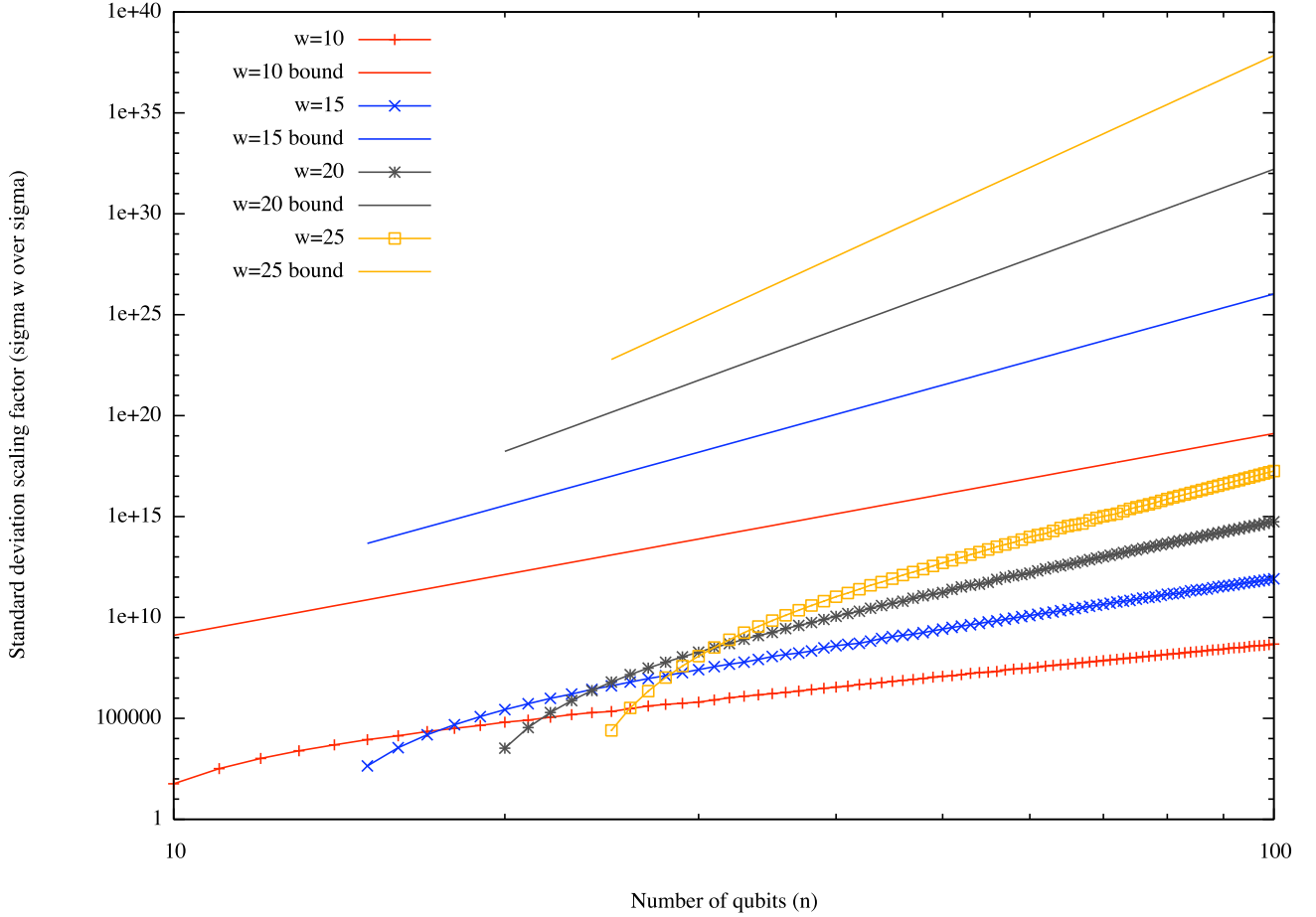


FIG. 5: Analytic upper bound on standard deviation scaling factor, and numerical calculations for scaling factor with worst case correlations.

where

$$k = -1.62521 \pm 0.09716 \quad (36)$$

$$a = 11.854 \pm 1.785 \quad (37)$$

$$m = 0.638924 \pm 0.0089 \quad (38)$$

$$b = -0.982147 \pm 0.1647. \quad (39)$$

APPENDIX D: METHODS

The two-qubit liquid-state experiments were performed on a sample made from 10mg of ^{13}C labeled chloroform (Cambridge Isotopes) dissolved in 0.51ml of deuterated acetone. The experiment was performed on a 700MHz Bruker Avance spectrometer using a dual inverse cryoprobe. The pulse programs were optimized on a home-built pulse sequence compiler which pre-simulates the pulses in an efficient pairwise manner and takes into account first order phase and coupling errors during a pulse by modifications of the refocussing scheme and pulse phases [29]. The solid-state experiments were performed on a single crystal of malonic acid which contained $\approx 7\%$ triply labeled ^{13}C molecules [30]. The experiments were performed at room temperature with a home-built probe. Apart from an initial polarization transfer, the protons were decoupled using the SPINAL64 sequence [31]. The required control fields that implemented the unitary propagators and state-to-state transformations were found using the GRAPE optimal control method [32] and made robust to inhomogeneities in both the r.f. and static fields. The implemented versions of the pulses were corrected for non-linearities in the signal generation and amplification process through a pickup

coil to measure the r.f. field at the sample and a simple feedback loop. The error probabilities for each experiment were calculated using a constrained maximum likelihood function.

Acknowledgements This work benefitted from discussions with R. Blume-Kohout, R. Cleve, D. Gottesman, E. Knill, B. Levi, and A. Nayak and technical expertise from M. Ditty. This research was supported by NSERC, MITACS, ORDCF, ARO and DTO.

-
- [1] Shor, P. W. Scheme for reducing decoherence in quantum computer memory. *Phys. Rev. A* **52**, R2493 (1995).
 - [2] Steane, A. M. Error correcting codes in quantum theory. *Phys. Rev. Lett.* **77**, 793 (1996).
 - [3] Shor, P. W., Fault-tolerant quantum computation. *Proceedings of the Symposium on the Foundations of Computer Science*, 56-65 (IEEE press, Los Alamitos, California, 1996).
 - [4] Aharonov, D. and Ben-Or, M., Fault-tolerant quantum computation with constant error. *Proceedings of the 29th Annual ACM Symposium on the Theory of Computing*, 176-188 (ACM Press, New York, New York, 1996).
 - [5] Kitaev, A. Y. Quantum computations: algorithms and error correction. *Uspekhi Mat. Nauk* **52**, 53-112 (1997).
 - [6] Knill, E., Laflamme, R., and Zurek, W. H. Resilient quantum computation. *Science* **279**, 342-345 (1998).
 - [7] Chuang, I. and Nielsen, M. *J. Mod. Opt.* **44**, 2455 (1997).
 - [8] D'Ariano, G. M. and Lo Presti, P. *Phys. Rev. Lett.* **86**, 4195 (2001).
 - [9] Mohseni, M. and Lidar, D. *Phys. Rev. Lett.* **97**, 170501 (2006).
 - [10] Haffner, H. *et al. Nature* **438**, 643 (2005).
 - [11] Leibfried, D. *et al. Nature* **438**, 639 (2005).
 - [12] Negrevergne, C. *et al.* Benchmarking quantum control methods on a 12-qubit system. *Phys. Rev. Lett.* **96**, 170501 (2006).
 - [13] Emerson, J. *et al.* Pseudo-Random Unitary Operators for Quantum Information Processing. *Science* **302**: 2098-2100 (2003).
 - [14] Levi, B. *et al.* Efficient Error Characterization in Quantum Information Processing, *Phys. Rev. A* **75**, 022314 (2007).
 - [15] Emerson, J., Alicki, R., Zyczkowski, K. *J. Opt. B: Quantum and Semiclassical Optics*, **7** S347-S352 (2005).
 - [16] Dankert, C. *et al.* submitted to *Phys. Rev. Lett.*, quant-ph/0606161 (2006).
 - [17] Dur, W. *et al. Phys. Rev. A* **72**, 052326 (2005).
 - [18] Cory, D.G. *et al.* NMR Based Quantum Information Processing: Achievements and Prospects. *Fortschritte der Physik* **48**, 875 - 907 (2000).
 - [19] Bennett, C. *et al. Phys. Rev. A* **54**(5), 3824-3851 (1996).
 - [20] Aliferis, P., Gottesman, D., Preskill, J. Quantum accuracy threshold for concatenated distance-3 codes. *Quant. Inf. Comp.* **6**, 97-165 (2006)
 - [21] Fortunato, E. M. *et al. J. Chem. Phys.* **116**, 7599-7606 (2002)
 - [22] Nielson, M., *Phys. Lett. A* **303** (4): 249-252 (2002).
 - [23] Knill, E. Scalable quantum computing in the presence of large detected-error rates. *Nature* **434**, 39-44 (2005).
 - [24] Knill, E. Quantum computing with realistically noisy devices. *Phys. Rev. A* **71**, 042322 (2005).
 - [25] The latter approach was suggested to us by E. Knill.
 - [26] Cory, D.G., Miller, J.B., and Garroway, A.N., Time-Suspension Multiple- Pulse Sequences: Applications to Solid-State Imaging. *Journal of Magnetic Resonance* **90**, 205-213 (1990).
 - [27] Haeberlen, U. *Advances in Magnetic Resonance*, Ed. J. Waugh, Academic Press, New York (1976).
 - [28] Boulant, N. *et al. Phys. Rev. A* **67**, 042322 (2003).
 - [29] Knill, E. *et al. Nature* **404**, 368-370 (2000).
 - [30] Baugh, J. *et al. Phys. Rev. A* **73**, 022305 (2006).
 - [31] Fung, B.M., Khitrin, A.K., Ermolaev, K., *Journal of Magnetic Resonance* **142**, 97-101 (2000).
 - [32] Khaneja, N., Reiss, T., Kehlet, C., Herbruggen, T.S., Glaser, S.J. *Journal of Magnetic Resonance* **172**, 296-305 (2005).